ACS APPLIED MATERIALS & INTERFACES

Research Article

www.acsami.org

Structure and Visible Light Luminescence of 3D Flower-like Co_3O_4 Hierarchical Microstructures Assembled by Hexagonal Porous Nanoplates

Wenzhong Wang* and Jie Xu

School of Science, Minzu University of China, Beijing 100081, China

ABSTRACT: A two-step strategy has been developed to fabricate 3D flower-like Co_3O_4 hierarchical microstructures assembled by hexagonal porous nanoplates. The synthetic procedure was described as (1) 3D flower-like α-$Co(OH)_2$ microstructures were prepared by a facile surfactant-free low-temperature hydrothermal process; (2) 3D flower-like Co_3O_4 hierarchical microstructures were fabricated by annealing the obtained 3D flower-like α-$Co(OH)_2$ microstructures. X-ray diffraction and Raman spectrum analyses demonstrate that the hierarchical microstructures formed from 3D flower-like α-$Co(OH)_2$ microstructures are composed of pure cubic phase Co_3O_4. Scanning electronic microscopy demonstrates that the as-prepared Co_3O_4 microstructures exhibit 3D flower-like hierarchical structures assembled by hexagonal porous nanoplates. Photoluminescence demonstrates that these novel 3D flower-like Co_3O_4 hierarchical microstructures display a broad strong emission in the visible range of 650 to 800 nm with a peak at around 710 nm (1.75 eV), which is very close to the indirect optical band gap of 1.60 eV for Co_3O_4 thin film. The result indicates that the photoluminescence emission likely originates from the indirect optical band gap emission. The broad photoluminescence emission may be resulted from a wide size distribution of porous nanoplates in 3D hierarchical microstructures. These 3D flower-like Co_3O_4 hierarchical microstructures with unique optical properties may find new potential applications in visible light emitting materials.

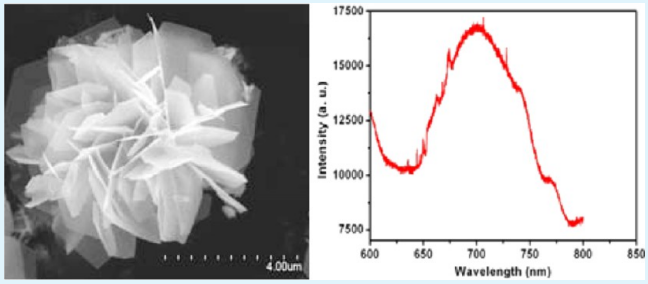

KEYWORDS: *three-dimensional hierarchical microstructures, two-dimensional porous nanoplates, low-temperature synthesis, visible light photoluminescence*

1. INTRODUCTION

Inorganic micro- and nanomaterials with controlled size and shape have recently attracted enormous attention owing to their strong physical properties for optical, electrical, and magnetic applications, which are very important for the development and realization of photoelectronic devices with high performance.[1] In addition, the assembly of the nano-building blocks into favored structures is also very important for the fabrication of nanodevices with advanced functions.[2] Therefore, it is highly desirable to study the physical properties of inorganic micro- and nanomaterials with controlled size and shape.

Cobalt oxide (Co_3O_4) is one of the most promising transition metal oxides due to its special structure with the direct optical band gap of around 2.10 eV and the indirect optical band gap of around 1.60 eV for thin film,[3,4] and potential applications in heterogeneous catalysts,[5] chemical gas sensors,[6] lithium-ion batteries[7,8] and magnetic materials,[9] quantum tunneling of magnetization,[10] supercapacitors,[11] and electrochromic devices.[12] Furthermore, it has been reported that Co_3O_4 micro- and nanostructures with controlled shape and size exhibit unique physical properties such as optical, magnetic, field emission and electrochemical properties. These unique properties are very attractive in the fabrication of Co_3O_4-based high-performance nanodevices.[13,14] Many efforts have therefore been inspired to study on the synthesis and properties of Co_3O_4 micro- and nanostructures. However, in recent years, enormous efforts have been mainly devoted to preparation and potential applications such as catalysts, gas sensors, and lithium-ion batteries,[5−8] but there are only a few reports on the investigations of physical properties such as optical and magnetic properties of Co_3O_4 micro- and nanostructures.[13,14] As is known, the design and fabrication of Co_3O_4-based photoelectronic nanodevices with advanced performance is greatly determined by the physical properties of Co_3O_4 micro- and nanostructures. Therefore, it is highly worthwhile to investigate the physical properties of Co_3O_4 micro- and nanostructures. Furthermore, the studies on physical properties of Co_3O_4 micro- and nanostructures can explore their new potential applications in optoelectronic nanodevices.

As was reported in the previous works, the shape and size of the Co_3O_4 micro- and nanostructures have an evident influence on their properties such as optical, magnetic, electrochemical

Received: September 17, 2014
Accepted: December 11, 2014
Published: December 11, 2014

properties, etc.[14,15] Thus, the control of the shape and size is a key issue to study the shape- and size-dependent properties of the Co_3O_4 micro- and nanostructures. So far, much research has been done on the synthesis and properties of Co_3O_4 micro- and nanostructures with controlled morphologies such as nanocubes,[16] nanorods,[17] nanosheets,[18] nanowires,[19] porous nanobelts,[20] hollow spheres, and flower-like nanostructures.[21,22]

In this work, three-dimensional (3D) flower-like Co_3O_4 hierarchical microstructures assembled by hexagonal porous nanoplates were successfully synthesized through annealing the 3D flower-like α-$Co(OH)_2$ microstructures, which were synthesized by a facile surfactant-free hydrothermal method. The structural features of the as-obtained Co_3O_4 hierarchical microstructures were characterized by scanning electron microscopy (SEM). Surface morphology observations show that the as-prepared Co_3O_4 hierarchical microstructures exhibit 3D flower-like structures assembled by dozens of two-dimensional (2D) nanoplates with a thickness of a few tens of nanometers. Characterizations of structural features reveal that 2D nanoplates display hexagonal porous structure. Furthermore, 3D Co_3O_4 hierarchical microstructures exhibit a strong broadened photoluminescence (PL) emission in the visible range of 650 to 800 nm with a maximum peak at 710 nm (1.75 eV). These Co_3O_4 hierarchical microstructures assembled by 2D hexagonal porous nanoplates are expected to find new potential applications in visible emitting materials, as well as sensors, optics and electronics.

The important novelty in the present study is the first report of 3D Co_3O_4 flower-like microstructures assembled by 2D hexagonal porous nanoplates. The as-fabricated 3D Co_3O_4 flower-like microstructures show unprecedented strong visible light PL emission when excited with a He−Cd laser at 325 nm. In addition, this work offers a facile strategy to fabricate 3D Co_3O_4 flower-like microstructures by annealing the obtained 3D flower-like α-$Co(OH)_2$ microstructures in large quantity.

2. EXPERIMENTAL SECTION

The 3D Co_3O_4 hierarchical microstructures assembled by 2D hexagonal porous nanoplates were fabricated by a two-step strategy. First, 3D flower-like α-$Co(OH)_2$ microstructures were synthesized by a facile surfactant-free hydrothermal process. In a typical procedure for the preparation of 3D flower-like α-$Co(OH)_2$ microstructures, 0.2 mmol of cobalt chloride ($CoCl_2 \cdot 6H_2O$), 1.0 mmol of sodium chloride (NaCl), and 1.2 mmol of hexamethylenetetramine (HMT) were dissolved in 200 mL of a mixture of deionized water and ethanol with volume ratio of 9:1 to give the final concentrations of 10, 50, and 60 mM, respectively. The reaction solution was stirred for 20 min and subsequently transferred into a 250 mL Teflon-sealed autoclave, sealed, and kept at 90 °C for 1 h in a furnace, and cooled to room temperature. The green precipitates were collected by centrifugation and subsequently washed with distilled water for several times, and then air-dried at room temperature.

Second, 3D Co_3O_4 hierarchical microstructures were fabricated by annealing the as-synthesized 3D flower-like α-$Co(OH)_2$ microstructures with the following procedure: the as-synthesized 3D flower-like α-$Co(OH)_2$ microstructures were heated in a porcelain crucible that was placed in the middle of an alumina tube with a horizontal tube electric furnace at 400 °C for 2 h, and the black powders were obtained by gradually cooling the heat-treated powders to room temperature in air.

X-ray powder diffraction (XRD) patterns were obtained on a Rigaku (Japan) D_{max} γ_A rotation anode X-ray diffractometer equipped with the graphite monochromatized Cu Kα radiation (λ = 1.541 78 Å), employing a scanning rate of 0.02° s^{-1} in the 2θ range from 10 to 80°. The structural features such as size and morphology were studied by scanning electron microscopy (SEM, Hitachi S-4800) and transmission electron microscopy (TEM, JEOL-2100), respectively.

The optical properties of the as-obtained nanostructures were investigated by PL and Raman spectra, which were performed on a LABRAM-HR confocal laser microRaman spectrometer at room temperature. The 325 nm line of a He−Cd laser with the capability of supplying 250 mW was used as the excitation source for the measurements of the PL and Raman spectra.

3. RESULTS AND DISCUSSION

The composition and crystallinity of the 3D flower-like α-$Co(OH)_2$ microstructures, fabricated by using a facile surfactant-free low-temperature hydrothermal process, were measured. Figure 1 is a typical XRD pattern of the $Co(OH)_2$

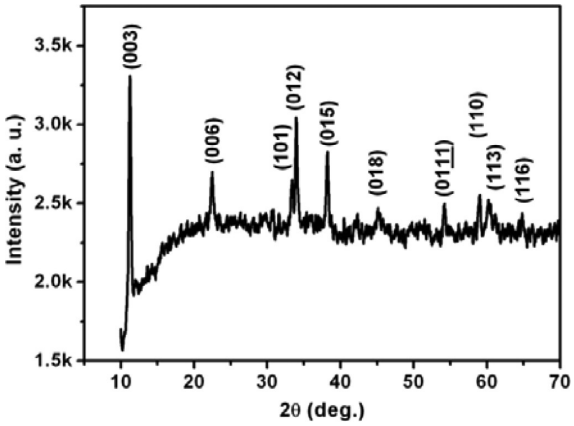

Figure 1. XRD pattern of the as-prepared 3D flower-like α-$Co(OH)_2$ microstructures.

precursors prepared by a facile surfactant-free hydrothermal process through heating the mixed solution of $CoCl_2$, NaCl, and HMT at 90 °C for 1 h. One can see from the XRD pattern that several characteristic diffraction peaks are observed. These diffraction peaks can be easily assigned on the basis of the crystal structure of α-$Co(OH)_2$ as reported before.[23,24] Four main characteristic diffraction peaks can be indexed to the (003), (006), (012), and (015) crystalline planes of α-$Co(OH)_2$. The diffraction peaks of β-$Co(OH)_2$ and cobalt oxides were not detected in the XRD pattern, indicating that pure phase α-$Co(OH)_2$ crystals are successfully synthesized via the present facile surfactant-free hydrothermal route. As reported in the previous research works, the pure phase α-$Co(OH)_2$ particle is difficult to synthesize compared to the β-$Co(OH)_2$ particle, because the α-$Co(OH)_2$ particle is metastable and can transform rapidly to the β-$Co(OH)_2$ during preparation or upon storage in strong alkaline media.[25] Therefore, our present study offers a new and facile surfactant-free hydrothermal route for the growth of stable α-$Co(OH)_2$ particle.

The morphology and size of the as-prepared α-$Co(OH)_2$ particles was estimated by SEM. Figure 2 shows SEM images of the as-obtained α-$Co(OH)_2$ particles with different magnifications. A typical low-magnification SEM image, as shown in Figure 2a, demonstrates that a large quantity of 3D flower-like microstructures was achieved. The size along diagonal axis of 3D flower-like microstructures is not uniform ranging from about 2 to 10 μm. Figure 2b is a typical medium-magnification SEM image of the as-obtained 3D flower-like α-$Co(OH)_2$ microstructures, showing that the microstructures are

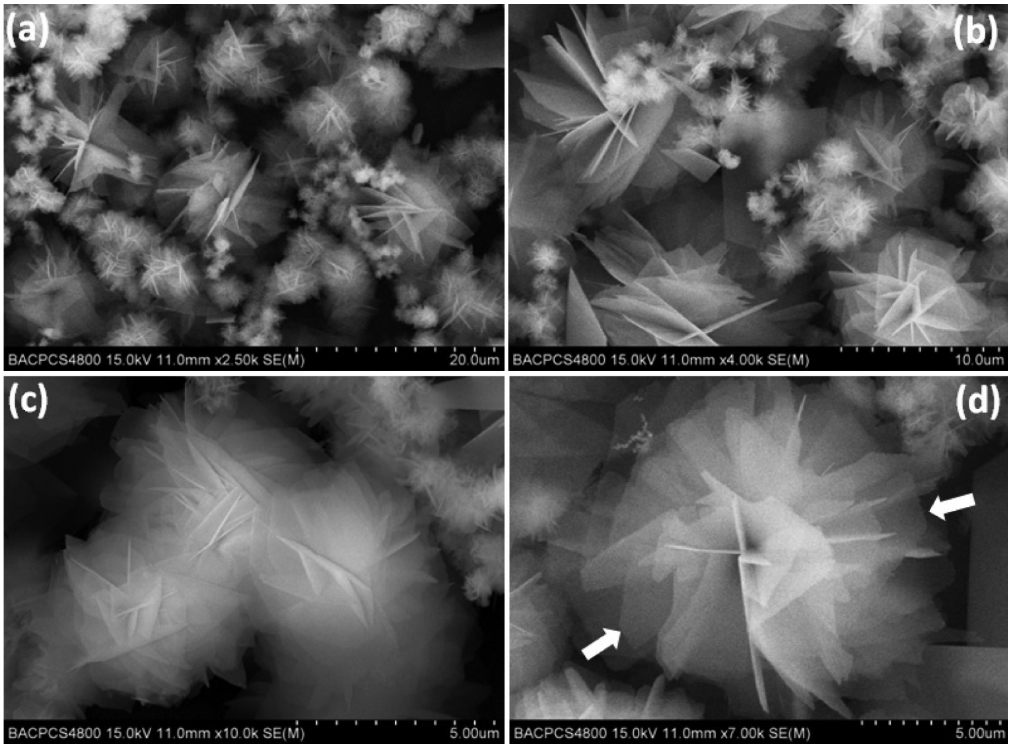

Figure 2. (a) Low-magnification SEM images of the as-synthesized 3D flower-like α-$Co(OH)_2$ microstructures. (b) Medium- and (c) high-magnification SEM images of 3D flower-like α-$Co(OH)_2$ microstructures, showing that the as-prepared microflowers are assembled by plate-like nanostructures. (d) SEM image of an individual microstructure, showing that 3D flower-like microstructures are assembled by many hexagonal nanoplates.

assembled by plate-like nanostructures. Higher magnification SEM images, as presented in Figure 2c, further confirm that the 3D flower-like microstructures are fabricated by self-assembly of nanoplates with thickness of a few tens of nanometers. Figure 2d shows a SEM image of an individual microstructure used to further study the structural features of the 3D flower-like microstructures. After a careful examination, one can find that 3D flower-like microstructure is assembled by hexagonal nanoplates as indicated by arrows in Figure 2d. The results of XRD and SEM demonstrate that 3D flower-like α-$Co(OH)_2$ microstructures assembled by hexagonal nanoplates can be successfully synthesized via the present facile surfactant-free hydrothermal method.

Figure 3 is the XRD diffraction pattern of the particles fabricated by annealing the 3D flower-like α-$Co(OH)_2$ microstructures at 400 °C for 2 h in air. The XRD pattern of the as-obtained particles exhibits several characteristic diffraction peaks that are in agreement with the standard PDF card (JCPDS 43-1003). One can find from the XRD pattern that the diffraction peaks are broadened, which may be resulted from the small size of the prepared particles. Five main characteristic diffraction peaks can be readily assigned to the (220), (311), (400), (511) and (440) planes of the cubic phase Co_3O_4 crystal with lattice constant a = 8.094 Å (JCPDS 43-1003). The diffraction peaks of other cobalt oxides and hydroxides are not detected in the XRD pattern. Thus, the result of XRD clearly demonstrates that the 3D flower-like α-$Co(OH)_2$ microstructures can be transformed to pure cubic phase Co_3O_4 crystals completely, after being annealed at 400 °C in air for 2 h.

The structural features of the as-synthesized Co_3O_4 crystals were investigated by SEM. Typical SEM images of the as-

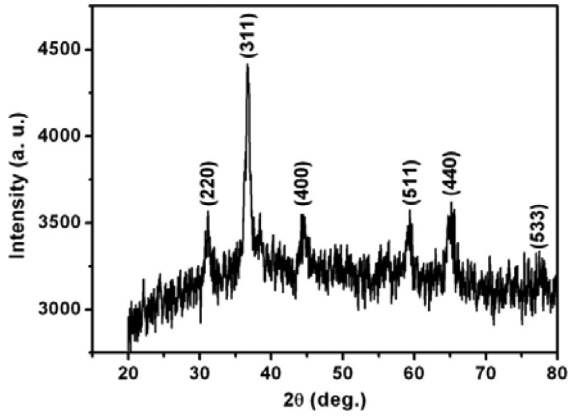

Figure 3. XRD pattern of the as-fabricated 3D flower-like Co_3O_4 hierarchical microstructures.

obtained Co_3O_4 crystals with different magnifications are shown in Figure 4. A typical low-magnification SEM image of the as-prepared Co_3O_4 crystals demonstrates that a large quantity of 3D flower-like hierarchical microstructures has been obtained, as shown in Figure 4a. These 3D flower-like hierarchical microstructures have diameters of around 2 to 10 μm, which is similar to those of 3D flower-like α-$Co(OH)_2$ precursors, as shown in Figure 2. Medium-magnification SEM image, as shown in Figure 4b, demonstrates that the entire flower-like hierarchical structures were assembled by many 2D nanoplates. Figure 4c is a typical SEM image of an individual 3D flower-like microstructure, clearly showing that the as-obtained 3D flower-like microstructure is built by many 2D hexagonal nanoplates, which is consistent with the morphology

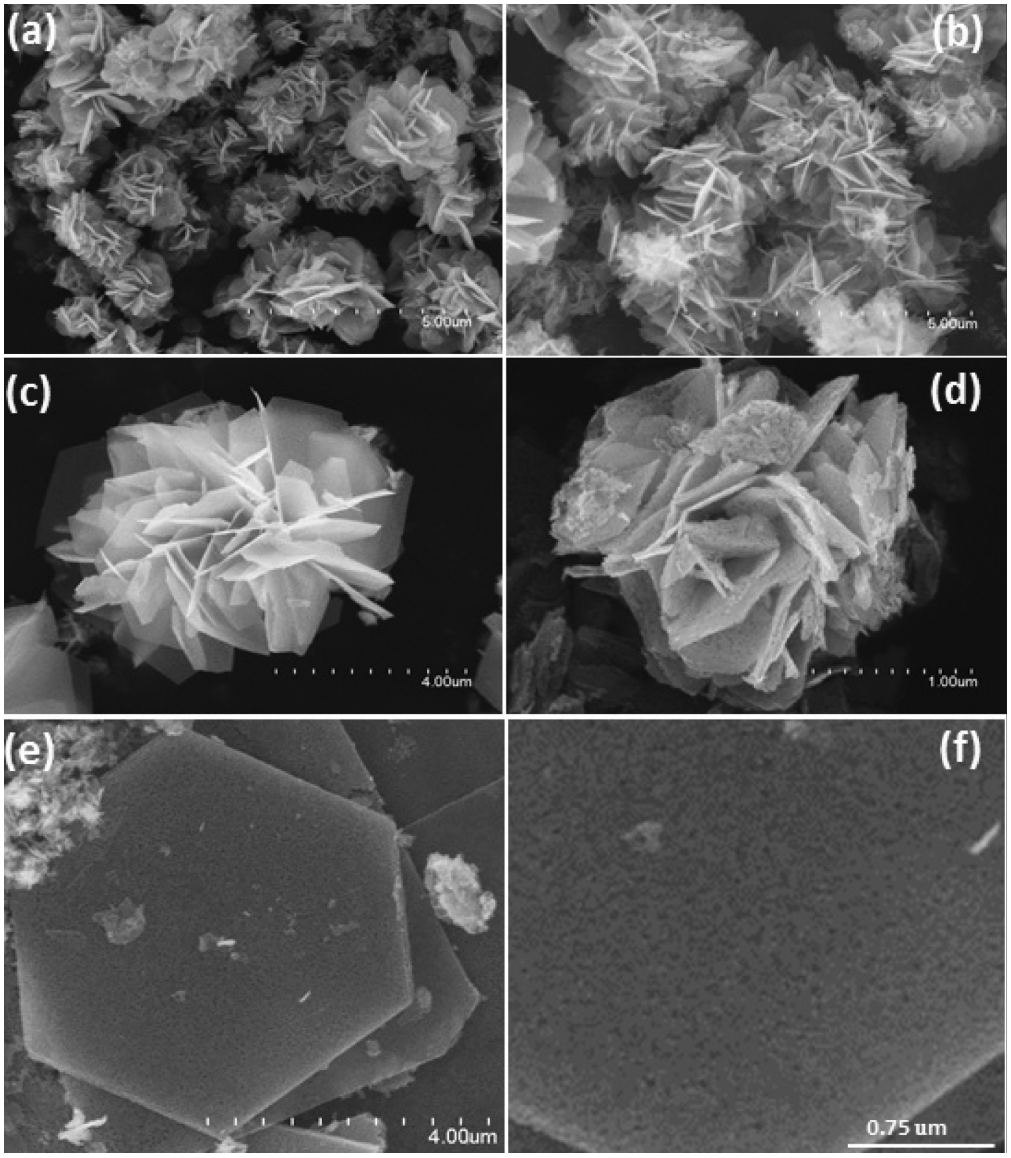

Figure 4. (a) Low- and (b) medium-magnification SEM images of 3D flower-like Co_3O_4 hierarchical microstructures. (c) SEM image of an individual microstructure, demonstrating that the nanostructure is assembled by many hexagonal nanoplates. (d) High-magnification SEM image of an individual nanostructure, showing that the nanostructure is assembled by many porous hexagonal nanoplates. (e and f) SEM image of an individual 2D hexagonal nanoplate and the corresponding enlarged SEM image, showing that the 2D hexagonal nanoplate exhibits a porous structure.

of 3D flower-like α-$Co(OH)_2$ precursors. Figure 4d is a typical high-magnification SEM image of a single flower-like hierarchical microstructure further used to exam its structural features. Interestingly, one can clearly find that the as-fabricated 3D flower-like hierarchical microstructures are composed of many hexagonal porous nanoplates. Figure 4e,f is a SEM image of an individual 2D hexagonal nanoplate and the corresponding enlarged SEM image used to study its structural feature. The enlarged SEM image clearly demonstrates that 2D hexagonal nanoplate exhibits porous structure.

The structural feature of the fabricated 3D flower-like Co_3O_4 microstructures was further studied by TEM. Figure 5 shows TEM images of the flower-like microstructures with different magnifications. Figure 5a demonstrates that the flower-like microstructures are built by 2D thin porous hexagonal nanoplates. The porous structural feature of the 2D nanoplates is further confirmed by a higher magnification TEM image of an individual hexagonal nanoplate, as shown in Figure 5b. One also can see from Figure 5b that the porous nanoplate is easily broken during the preparation of the TEM sample. Thus, the results of XRD, SEM, and TEM demonstrate that the novel 3D flower-like Co_3O_4 microstructures assembled by many 2D porous hexagonal nanoplates can be successfully fabricated by the present strategy.

It is desirable to give a rational interpretation for the roles of NaCl and HMT in the formation of the 3D α-$Co(OH)_2$ flower-like microstructures. As was reported in the previous literature,[26−28] HMT decomposed into formaldehyde and ammonia in aqueous deposition baths. In addition, it also has been reported that NaCl can be used to increase the rate of nanoparticle self-assembly;[29] these works offer us reasonable suggestions for the roles of NaCl and HMT, and the growth mechanism of 3D α-$Co(OH)_2$ flower-like microstructures. During the hydrothermal process at 90 °C, HMT gradually

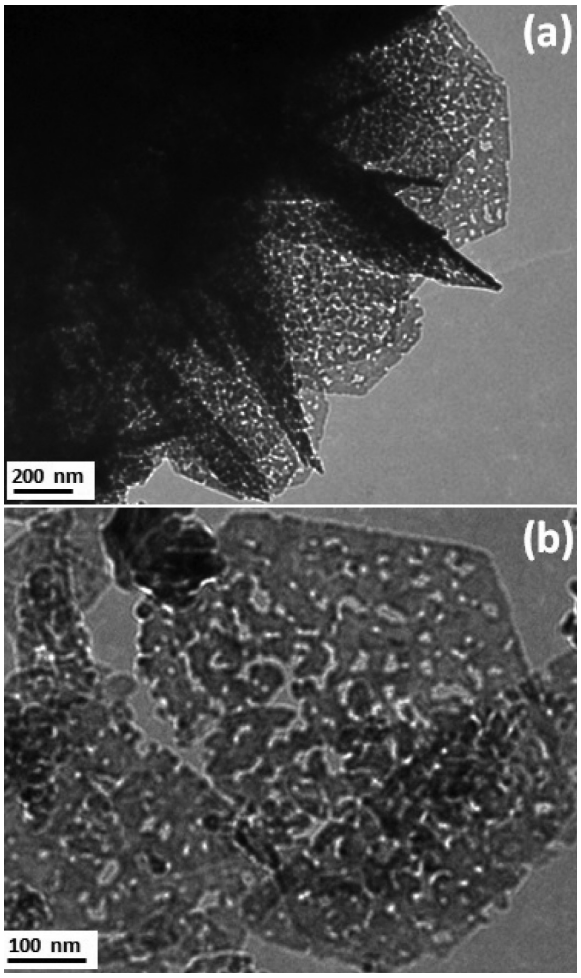

Figure 5. (a) Low- and (b) high-magnification TEM images of the as-fabricated 3D flower-like Co_3O_4 microstructures.

decomposes into formaldehyde and ammonia in the reaction aqueous, then the newly formed ammonia reacts with water to produce OH^-. Second, Co^{2+} reacts with OH^- to form α-$Co(OH)_2$ crystal nuclei, the newly formed α-$Co(OH)_2$ crystal nuclei grow into 2D plate-like nanocrystals with the aid of NaCl. In addition, the layer structural feature of α-$Co(OH)_2$ crystal also makes it nuclei to grow into 2D plate-like nanocrystals. Finally, the plate-like α-$Co(OH)_2$ nanocrystals assemble to form 3D flower-like microstructures by spiral assembly with the assistance of NaCl. In the growth of 3D α-$Co(OH)_2$ flower-like microstructures, the HMT offers OH^- by releasing ammonia in the reaction aqueous. NaCl may assist the plate-like α-$Co(OH)_2$ nanocrystals to assemble into 3D flower-like microstructures, although the exact role of NaCl is not very clear and need to study further. The chemical reaction for the formation of flower-like α-$Co(OH)_2$ microstructures can be formulated as[26]

$$(CH_2)_6N_4 + H_2O \rightarrow 6HCHO + NH_3 \quad (1)$$

$$NH_3 + H_2O \leftrightarrow NH^{4+} + OH^- \quad (2)$$

$$Co^{2+} + 2OH^- \rightarrow Co(OH)_2 \quad (3)$$

The study of the optical property of the Co_3O_4 micro- and nanostructures is very important for the design and fabrication of Co_3O_4-based nanodevices. On the other hand, it has been demonstrated that Co_3O_4 micro- and nanostructures with controlled shape and size exhibit unique physical properties. In this study, we have used Raman and PL spectroscopy to estimate the optical properties of the as-obtained 3D flower-like Co_3O_4 hierarchical microstructures assembled by hexagonal porous nanoplates. In addition, the composition and structural features of the as-prepared hierarchical microstructures were further identified by Raman spectroscopy, because Raman spectroscopy, a nondestructive characterization technique, is an effective method for the studies of the vibrational properties and microstructure features of micro- and nanostructures.[30,31] Figure 5 shows a typical Raman spectrum of the as-obtained 3D flower-like Co_3O_4 hierarchical microstructures assembled by hexagonal porous nanoplates. The spectrum was taken with a LABRAM-HR confocal laser microRaman spectrometer using a 325 nm He−Cd laser as the excitation source at room temperature. One can find that only one Raman peak at about 580 cm^{-1} is observed. The peak can be indexed to the F^3_{2g} mode of the crystalline Co_3O_4.[32,33] No vibrational modes of CoO[34] are detected in the Raman spectrum of the as-obtained 3D hierarchical microstructures. Thus, on the basis of the results of XRD and Raman spectrum, it is reasonable to conclude that the as-prepared 3D flower-like hierarchical microstructures assembled by hexagonal porous nanoplates are pure cubic phase Co_3O_4.

It is known that the optical property of semiconductor micro- and nanomaterials, including band gap determination, impurity levels and defect detection, and recombination mechanisms of photoinduced carries in semiconductor micro- and nanoparticles, is widely investigated by PL spectroscopy. A typical room temperature PL spectrum of the as-prepared 3D flower-like Co_3O_4 hierarchical microstructures assembled by hexagonal porous nanoplates is shown in Figure 6, showing that

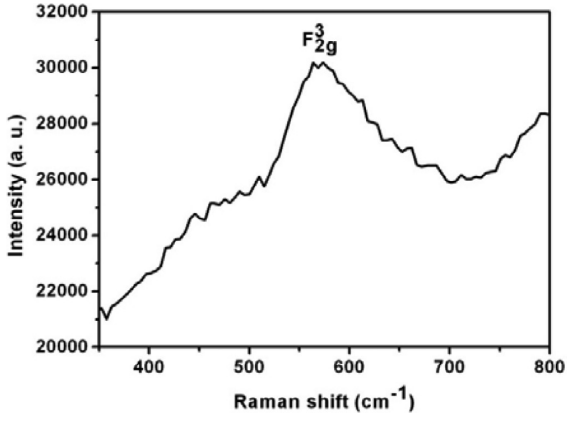

Figure 6. Room-temperature Raman spectrum of the as-synthesized 3D flower-like Co_3O_4 hierarchical microstructures under the 325 nm laser excitation.

the as-obtained hierarchical microstructures emit stably visible light at room temperature, when excited with a 325 nm He−Cd laser. One can clearly see that the PL spectrum exhibits a strong emission in the visible light range of 650 to 800 nm centered at about 710 nm, which corresponds to an energy of 1.75 eV. The value is very close to the indirect optical band gap of 1.60 eV, as reported for Co_3O_4 thin film.[3,4] Thus, the PL peak of the as-prepared 3D flower-like Co_3O_4 hierarchical microstructures likely originates from the indirect optical band gap emission.[3,4] In addition to strong visible light emission, the emission peak in

dx.doi.org/10.1021/am506414n | ACS Appl. Mater. Interfaces 2015, 7, 415−421

PL spectrum of the obtained hierarchical microstructures is broadened significantly as shown in Figure 6. It has been demonstrated that the size and morphology of the micro- and nanocrystal have a great effect on its energy band gap.[35] In the present case, the as-obtained 3D flower-like Co_3O_4 hierarchical microstructures assembled by hexagonal porous nanoplates display a wide distribution in diameter. These structure features make the as-obtained Co_3O_4 hierarchical microstructures to exhibit a distribution of the energy band gaps, which is responsible for the broad emission in the PL spectrum. Similar broad PL emission feature has been reported in Co_3O_4 nanorods[36] and nanowires.[37] The unique optical properties exhibited by the as-achieved 3D flower-like Co_3O_4 hierarchical microstructures assembled from hexagonal porous nanoplates may make these micromaterials to find new potential applications in visible light emitting materials (Figure 7).

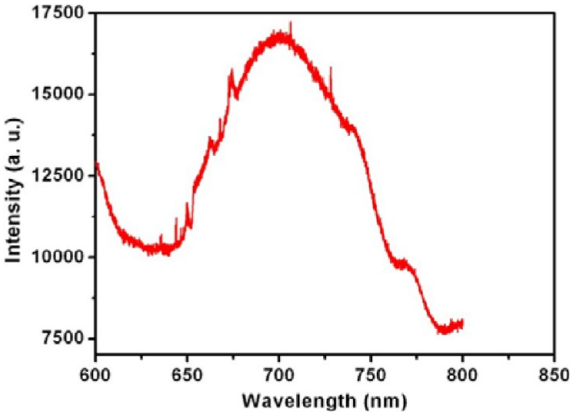

Figure 7. Room-temperature PL spectrum of the as-synthesized 3D flower-like Co_3O_4 hierarchical nanostructures under the 325 nm laser excitation.

4. CONCLUSIONS

3D flower-like Co_3O_4 hierarchical microstructures assembled by hexagonal porous nanoplates have been successfully prepared by annealing the 3D flower-like α-$Co(OH)_2$ microstructures, which were synthesized through a facile and simple surfactant-free hydrothermal method. The composition and crystallization phase of the as-obtained Co_3O_4 hierarchical microstructures were studied by X-ray diffraction and Raman spectrum. The results demonstrate that the as-prepared hierarchical microstructures are composed of pure cubic phase Co_3O_4. The structural features such as morphology and size of the obtained hierarchical microstructures were studied by scanning electronic microscopy and transmission electron microscopy. The results show that the as-prepared Co_3O_4 microstructures exhibit novel 3D flower-like hierarchical structures assembled by hexagonal porous nanoplates and display a wide distribution in diameter. Photoluminescence investigation shows that these novel 3D flower-like Co_3O_4 hierarchical microstructures built with hexagonal porous nanoplates exhibit a broad strong emission in the visible range of 650 to 800 nm with a peak at around 710 nm (1.75 eV). The value is very close to the indirect optical band gap of 1.60 eV for Co_3O_4 thin film; therefore, the photoluminescence peak likely originates from the indirect optical band gap emission. An ununiform shape and a wide size distribution of porous nanoplates in 3D hierarchical microstructures may result in a broad photoluminescence emission. The unique optical properties demonstrated by the as-obtained 3D flower-like Co_3O_4 hierarchical microstructures may lead them to potential applications in visible light emitting materials.

AUTHOR INFORMATION

Corresponding Author

*W. Z. Wang. E-mail: wzhwangmuc@163.com. Tel: 010-68930239.

Notes

The authors declare no competing financial interest.

ACKNOWLEDGMENTS

This work was supported by the National Natural Science Foundation of China under Grant Nos 11074312 and 11374377), and the Undergraduate Innovative Test Program of China under Grant Nos GCCX2013110004 and GCCX2014110010, and the Undergraduate Research Training Program of Minzu University of China under Grant Nos. URTP2013110039 and URTP2014110038.

REFERENCES

(1) Schlegel, G.; Bohnenberger, J.; Potapova, I.; Mews, A. Fluorescence Decay Time of Single Semiconductor Nanocrystals. *Phys. Rev. Lett.* **2002**, *88*, 137401.

(2) Breen, T. L.; Tien, J.; Oliver, S. R. J.; Hadzic, T.; Whitesides, G. M. Design and Self-Assembly of Open, Regular, 3D Mesostructures. *Science* **1999**, *284*, 948−951.

(3) Shinde, V. R.; Mahadik, S. B.; Gujar, T. P.; Lokhande, C. D. Supercapacitive Cobalt Oxide (Co_3O_4) Thin Films by Spray Pyrolysis. *Appl. Surf. Sci.* **2006**, *252*, 7487−7492.

(4) Gulino, A.; Fiorito, G.; Fragalá, I. Deposition of Thin Films of Cobalt Oxides by MOCVD. *J. Mater. Chem.* **2003**, *13*, 861−865.

(5) Liotta, L. F.; Carlo, G. D.; Pantaleo, G.; Deganello, G. Co_3O_4/CeO_2 and Co_3O_4/CeO_2-ZrO_2 Composite Catalysts for Methane Combustion: Correlation between Morphology Reduction Properties and Catalytic Activity. *Catal. Commun.* **2005**, *6*, 329−336.

(6) Nam, H. J.; Sasaki, T.; Koshizaki, N. J. Optical CO Gas Sensor Using a Cobalt Oxide Thin Film Prepared by Pulsed Laser Deposition under Various Argon Pressures. *J. Phys. Chem. B* **2006**, *110*, 23081−23084.

(7) Li, W. Y.; Xu, L. N.; Chen, J. Co_3O_4 Nanomaterials in Lithium-Ion Batteries and Gas Sensors. *Adv. Funct. Mater.* **2005**, *15*, 851−857.

(8) Chen, J. S.; Zhu, T.; Hu, Q. H.; Gao, J. F.; Su, F. B.; Qiao, S. Z.; Lou, X. W. Shape-Controlled Synthesis of Cobalt-based Nanocubes, Nanodiscs, and Nanoflowers and Their Comparative Lithium-Storage Properties. *ACS Appl. Mater. Interfaces* **2010**, *2*, 3628−3635.

(9) Wang, Y. Q.; Yang, C. M.; Schmidt, W.; Spliethoff, B.; Bill, E.; Schuth, F. Weakly Ferromagnetic Ordered Mesoporous Co_3O_4 Synthesized by Nanocasting from Vinyl-Functionalized Cubic *Ia3d* Mesoporous. *Adv. Mater.* **2005**, *17*, 53−56.

(10) Calderia, A. O.; Leggett, A. J. Influence of Dissipation on Quantum Tunneling in Macroscopic Systems. *Phys. Rev. Lett.* **1981**, *46*, 211−214.

(11) Deori, K.; Ujjain, S. K.; Sharm, R. K.; Deka, S. Morphology Controlled Synthesis of Nanoporous Co_3O_4 Nanostructures and Their Charge Storage Characteristics in Supercapacitors. *ACS Appl. Mater. Interfaces* **2013**, *5*, 10665−10672.

(12) Xia, X. H.; Tu, J. P.; Zhang, J.; Xiang, J. Y.; Wang, X. L.; Zhao, X. B. Cobalt Oxide Ordered Bowl-like Array Films Prepared by Electrodeposition through Monolayer Polystyrene Sphere Template and Electrochromic Properties. *ACS Appl. Mater. Interfaces* **2010**, *2*, 186−192.

(13) Wang, R. M.; Liu, C. M.; Zhang, H. Z.; Chen, C. P.; Guo, L.; Xu, H. B.; Yang, S. H. Porous Nanotubes of Co_3O_4: Synthesis,

Characterization, and Magnetic Properties. *Appl. Phys. Lett.* **2004**, *85*, 2080.
(14) Wang, X.; Chen, X. Y.; Gao, L. S.; Zhang, H. G.; Zhang, Z.; Qian, Y. T. One-Dimensional Arrays of Co_3O_4 Nanoparticles: Synthesis, Characterization, and Optical and Electrochemical Properties. *J. Phys. Chem. B* **2004**, *108*, 16401−16464.
(15) Feng, J.; Zeng, H. C. Size-Controlled Growth of Co_3O_4 Nanocubes. *Chem. Mater.* **2003**, *15*, 2829−2835.
(16) Hu, L. H.; Sun, K. Q.; Peng, Q.; Xu, B. Q.; Li, Y. D. Surface Active Sites on Co_3O_4 Nanobelt and Nanocube Model Catalysts for CO Oxidation. *Nano Res.* **2010**, *3*, 363−368.
(17) Xie, X. W.; Shang, P. J.; Liu, Z. Q.; Lv, Y. G.; Li, Y.; Shen, W. J. Synthesis of Nanorod-Shaped Cobalt Hydroxycarbonate and Oxide with the Mediation of Ethylene Glycol. *J. Phys. Chem. C* **2010**, *114*, 2116−2123.
(18) Hu, L. H.; Peng, Q.; Li, Y. D. Selective Synthesis of Co_3O_4 Nanocrystal with Different Shape and Crystal Plane Effect on Catalytic Property for Methane Combustion. *J. Am. Chem. Soc.* **2008**, *130*, 16136−16137.
(19) Tian, B. Z.; Liu, X. Y.; Yang, H. F.; Xie, S. H.; Yu, C. Z.; Zhao, D. Y. General Synthesis of Ordered Crystallized Metal Oxide Nanoarrays Replicated by Microwave-Digested Mesoporous Silica. *Adv. Mater.* **2003**, *15*, 1370−1374.
(20) Huang, H.; Zhu, W. J.; Tao, X. Y.; Xia, Y.; Yu, Z. Y.; Fang, J. W.; Gan, Y. P.; Zhang, W. K. Nanocrystal-Constructed Mesoporous Single-Crystalline Co_3O_4 Nanobelts with Superior Rate Capability for Advanced Lithium-Ion Batteries. *ACS Appl. Mater. Interfaces* **2012**, *4*, 5974−5980.
(21) Zhao, Z. G.; Geng, F. X.; Bai, J. B.; Cheng, H. M. Facile and Controlled Synthesis of 3D Nanorods-based Urchinlike and Nanosheets-based Flowerlike Cobalt Basic Salt Nanostructures. *J. Phys. Chem. C* **2007**, *111*, 3848−3852.
(22) Zheng, J.; Liu, J.; Lv, D. P.; Kuang, Q.; Jiang, Z. Y.; Xie, Z. X.; Huang, R. B.; Zheng, L. S. A Facile Synthesis of Flower-like Co_3O_4 Porous Spheres for the Lithium-Ion Battery Electrode. *J. Solid State Chem.* **2010**, *183*, 600−605.
(23) Oaki, Y.; Kajiyama, S.; Nishimura, T.; Kato, T. Selective Synthesis and Thin-Film Formation of α-Cobalt Hydroxide through an Approach Inspired by Biomineralization. *J. Mater. Chem.* **2008**, *18*, 4140−4142.
(24) Yang, J.; Liu, H. W.; Martens, W. N.; Frost, R. L. Synthesis and Characterization of Cobalt Hydroxide, Cobalt Oxyhydroxide, and Cobalt Oxide Nanodiscs. *J. Phys. Chem. C* **2010**, *114*, 111−119.
(25) Gaunand, A.; Lim, W. L. From Amorphous Precipitates to Sub-Micronic Crystalline Platelets of $Co(OH)_2$: A Kinetic Study of the Transformation Process. *Powder Technol.* **2002**, *128*, 332−337.
(26) Chng, Y. C.; Hutagalung, S. D. Gas Sensing Behavior of Zinc Oxide Nanorods Synthesized via Hydrothermal Method. *Solid State Sci. Technol.* **2011**, *19*, 162−169.
(27) Govender, K.; Boyle, D. S.; Kenway, P. B.; O'Brien, P. Understanding the Effects that Govern the Deposition and Morphology of This Films of ZnO from Aqueous Solution. *J. Mater. Chem.* **2004**, *14*, 2575−2591.
(28) McBride, R. A.; Kelly, J. M.; McCormack, D. E. Growth of Well-Defined ZnO Microparticles by Hydroxide Ion Hydrolysis of Zinc Salts. *J. Mater. Chem.* **2003**, *13*, 1196−1201.
(29) Liu, k.; Resetco, C.; Kumacheva, E. Salt-Mediated Kinetics of the Self-Assembly of Gold Nanorods End-Tethered with Polymer Ligands. *Nanoscale* **2012**, *4*, 6574−6580.
(30) Yan, B.; Chen, R.; Zhou, W. W.; Zhang, J. X.; Sun, H. D.; Gong, H.; Yu, T. Localized Suppression of Longitudinal-Optical-Phonon-Exciton Coupling in Bent ZnO Nanowires. *Nanotechnology* **2010**, *21*, 445706.
(31) Sahoo, S.; Harma, G. L. S.; Katiyar, R. S. Raman Spectroscopy to Probe Residual Stress in ZnO Nanowire. *J. Raman Spectrosc.* **2012**, *43*, 72−75.
(32) Hadjiev, V. G.; Iliev, M. N.; Vergilov, I. V. Raman Spectra of Co_3O_4. *J. Phys. C: Solid State Phys.* **1998**, *21*, L199.
(33) Yu, T.; Zhu, Y.; Xu, X.; Shen, Z.; Chen, P.; Lim, C. T.; Thing, J. T. L.; Sow, C. H. Controlled Growth and Field-Emission Properties of Cobalt Oxide Nanowalls. *Adv. Mater.* **2005**, *17*, 1595−1599.
(34) Chou, H. H.; Fan, H. Y. Light Scattering by Magnons in CoO, MnO, and α-MnS. *Phys. Rev. B* **1976**, *13*, 3924.
(35) Brus, L. E. Electro-Electron and Electron-Hole Interactions in Small Semiconductor Crystallites: The Size Dependence of the Lowest Excited Electronic State. *J. Chem. Phys.* **1984**, *80*, 4403.
(36) He, L.; Li, Z. C.; Zhang, Z. J. Rapid, Low-Temperature Synthesis of Single-Crystalline Co(3)O(4) Nanorods on Silicon Substrates on a Large Scale. *Nanotechnology* **2008**, *19*, 155606.
(37) Dong, Z.; Fu, Y. Y.; Han, Q.; Xu, Y. Y.; Zhang, H. Synthesis and Physical Properties of Co_3O_4 Nanowires. *J. Phys. Chem. C* **2007**, *111*, 18475−18478.